Rock and Soil Mechanics

Volume 41 | Issue 2 Article 7

9-27-2020

Effective stress yielding behavior of unsaturated loess under true triaxial conditions

Jin-jin FANG
School of Civil Engineering，Henan Polytechnic University, Jiaozuo, Henan 454000, China

Yi-xin FENG
Capital Construction Department, Henan Polytechnic University, Jiaozuo, Henan 454000, China, 327256272@qq.com

Li-ping WANG
School of Civil Engineering，Henan Polytechnic University, Jiaozuo, Henan 454000, China

Yong-qiang YU
School of Civil Engineering，Henan Polytechnic University, Jiaozuo, Henan 454000, China

Follow this and additional works at: https://rocksoilmech.researchcommons.org/journal

 Part of the Geotechnical Engineering Commons

Custom Citation

FANG Jin-jin, FENG Yi-xin, WANG Li-ping, YU Yong-qiang, . Effective stress yielding behavior of unsaturated loess under true triaxial conditions[J]. Rock and Soil Mechanics, 2020, 41(2): 492-500.

This Article is brought to you for free and open access by Rock and Soil Mechanics. It has been accepted for inclusion in Rock and Soil Mechanics by an authorized editor of Rock and Soil Mechanics.

Rock and Soil Mechanics 2020 41(2): 492−500 ISSN 1000−7598
https: //doi.org/10.16285/j.rsm.2019.5351 rocksoilmech.researchcommons.org/journal

Effective stress yielding behavior of unsaturated loess under true triaxial conditions

FANG Jin-jin[1], FENG Yi-xin[2], WANG Li-ping[1], YU Yong-qiang[1]
1. School of Civil Engineering，Henan Polytechnic University, Jiaozuo, Henan 454000, China
2. Capital Construction Department, Henan Polytechnic University, Jiaozuo, Henan 454000, China

Abstract: To study yield characteristics of unsaturated loess in the effective stress space, a series of undrained isotropic net stress compression consolidation and shear tests with different intermediate principal stress parameters b is conducted on unsaturated intact loess by using true triaxial apparatus. The effective stress yielding behaviors of unsaturated loess under true triaxial compression conditions are studied. The results show that the effective stress ratio decreases with an increase in intermediate principal stress or net confining pressure, and the effect of intermediate principal stress on effective spherical stress is greater than on the generalized shear stress. The yield curves determined by the effective stress ratio-volume strain curves have good regularity in the effective stress space, the effective yield stress at yield point increases with an increase in intermediate principal stress and initial suction. The effective stress yield strength surfaces and the strength failure surfaces on the π plane are in good agreement with the SMP strength criterion. As the effective spherical stress and initial suction are larger, the yield strength surface and strength failure surface are more larger. The equations of elastic shear strain and plastic shear strain under true triaxial conditions are proposed. By analyzing the relationship between effective stress and plastic strain, it is concluded that the plastic potential surfaces on different meridian planes in the effective stress space are elliptical, and the elliptical yield surface increases with an increase in intermediate principal stress.
Keywords: unsaturated intact loess; effective stress; yield; plastic potential surface

1 Introduction

Unsaturated soils are composed of solid, liquid and gas phases, and their properties are more complex than saturated soils. Unsaturated soils are widely used in engineering, thus many scholars have done a great deal of researches on their mechanical properties. Effective stress research is the basis and premise for studies on mechanical properties of unsaturated soils. Especially after Terzaghi[1] put forward the effective stress formula of saturated soil and the successful applications of effective stress principle, effective stress has received widespread attention from scholars both domestic and abroad [2−11]. Based on the effective stress concept of saturated soil, Bishop[2] put forward the effective stress formula of unsaturated soil, which is a formula of single stress variable. It has the advantages of simple formula and easy to grasp, and has been widely applied in engineering field. Jennings et al.[3] found that all the samples exhibited characteristics of collapsibility in the wetting process (i.e., the stage of suction reduction), through the consolidation experiment of unsaturated soil. However, the calculation of single stress variable effective stress formula proposed by Bishop[2] would obtain the result of expansion, which was obviously not consistent with the fact. Therefore, Jennings et al.[3] questioned the effective stress of single stress variable, that it could not describe the collapsibility phenomenon of unsaturated soil in the humidification process. Thus, Coleman[4], Bishop et al.[5−6] proposed two independent stress variables of net stress and matric suction to describe the strength and deformation of unsaturated soils. Fredlund et al.[7] verified the validity of double stress variables by zero position tests. Since then, the double stress variables have developed rapidly and been dominant in the study of unsaturated soil mechanics for a long time. However, Wheeler et al.[8] pointed out that the properties of unsaturated soil are not only affected by the net stress and matric suction, but also other factors such as the degree of saturation. Even though the net stress, matric suction and void ratio are the same, the mechanical properties of soils with different degrees of saturation and the interaction between soil particles (the so-called effective stress) are different. This shows that the strength and deformation of unsaturated soil cannot be determined by using only two independent stress variables. Subsequently Bolzon et al.[9] replaced the Bishop effective stress parameter χ with the degree of saturation S_r from the perspective of soil mechanics, and defined the effective average stress (i.e. the average soil skeleton stress) of unsaturated soil as:

Received：13 Feburary 2019 Revised：8 May 2019
This work was supported by the National Natural Science Foundation of China(51808197, 51704097), the Doctorate Fund of Henan Polytechnic University (B2018-64) and the Key Research Project of Colleges and Universities in Henan Province (19A560010).
First author: FANG Jin-jin, female, born in 1984, PhD, Lecturer. Research interests: soil mechanics of loess. E-mail: 286137393@qq.com
Corresponding author: FENG Yi-xin, male, born in 1985, Master, Engineer. Research interests: soil mechanics of loess. E-mail: 327256272@qq.com

$$p' = p + S_r s \quad (1)$$

where p is the net mean stress; S_r is the saturation; s is the suction.

Miao[10] established a constitutive model of unsaturated soil according to the effective stress Eq. (1) proposed by Bolzon et al.[9]. Sun [11] used Eq. (1) to represent the average soil skeleton stress and established the constitutive model of unsaturated soil by comprehensively considering the two stress variables and degree of saturation. Chen et al.[12] used Eq. (1) to express the effective mean stress, and studied the critical state characteristics of undisturbed loess in the p'-q and e-lnp' planes under conventional triaxial shear condition. The above results [10–12] are all based on the conventional triaxial stress conditions, without considering the influence of intermediate principal stress on soil strength and deformation. At present, there are few true triaxial test reports on the change law of effective stress yield conditions of unsaturated loess. The stress on the soil skeleton directly affects the deformation and strength of soil. Therefore, based on the effective stress Eq. (1) proposed by Bolzon et al. [9], this paper studied the change laws of the effective stress yield of unsaturated intact loess. Utilizing true triaxial apparatus, the effect of intermediate principal stress on the effective stress and yield characteristics of the unsaturated loess are discussed. And some theoretical basis are provided for the development of effective stress for unsaturated soil.

2 Test apparatus and methods

2.1 Test apparatus

The test apparatus adopted the true triaxial apparatus of Xi'an University of Technology, which can independently apply three-dimensional principal stresses to the specimen and measure the three-dimensional strains and volumetric strain. The true triaxial instrument was modified to meet the requirements of unsaturated soil test. Pore gas pressure controlling and measuring devices were added at the connecting position of the sample cap, so that air pressure could be uniformly applied to the sample. Clay plate was added to the pressure chamber base, which allowed water to pass but not gas when saturated. A high-precision sensor was connected to the base of the instrument for measuring the pore water pressure of the sample. The matric suction was the applied air pressure minus the measured pore water pressure . The details of instrument structure were described in the literature [13–15].

2.2 Sample preparation and test methods

The test samples are Q_3 undisturbed loess in Xi'an, Shaanxi province of China. Samples are from 8 m below the surface. The basic physical properties of the sample are listed in Table 1. The soil sample is cut into 7 cm×7 cm×14 cm according to the preparation method of intact sample. In accordance with the geotechnical testing rules, four different moisture contents are prepared at 12.8%, 16.1%, 17.8% and 20.3%. The corresponding initial suction s_0 under stress-free conditions are 455 kPa, 170 kPa, 92 kPa and 46 kPa, respectively.

During the test, the drainage valve on the base of the instrument is always closed and set to undrained condition. During the consolidation process, the net confining pressure σ_3 are 50kPa, 100kPa, 200kPa and 300kPa, respectively. The method of strain loading is adopted in the shear test and the intermediate principal stress parameter b (b = 0, 0.25, 0.5, 0.75, 1) is a constant. Which is, when the net confining pressure is constant, the shear tests with five different intermediate principal stress parameter b values are carried out, respectively. The shear rate is 0.005mm/min. Specific loading and test methods are described in the literature [14–15].

Table 1 Physical properties of specimen

Relative density, G_s	Moisture content, w_0 / %	Dry density ρ_d / (g·cm^{-3})	Void ratio, e_0	Liquid limit, w_L / %	Plastic limit, w_p / %
2.7	16.1	1.345	1.007	31.67	20.91

3 Analysis of test results

3.1 Effective stress-strain relationship of unsaturated soil

3.1.1 The relationship between effective stress ratio and generalized shear strain

The expression of generalized shear stress q is as follows:

$$q = \frac{1}{\sqrt{2}}\sqrt{\left[(\sigma_1-\sigma_2)^2+(\sigma_2-\sigma_3)^2+(\sigma_3-\sigma_1)^2\right]} \quad (2)$$

Figure 1 shows the (q/p') - ε_s relationship curves between effective stress ratio (q/p') and generalized shear strain ε_s of unsaturated intact loess with initial suction s_0 = 170 kPa. When the net confining pressure σ_3 is constant, the effective stress ratios at different b values all increase with the increase of generalized shear strain. The (q/p') – ε_s curves show a downward trend with the increase of b value, that is when ε_s is constant, the effective stress ratio reduces with the increase of b value. This indicates that the effect of intermediate principal stress increase on the effective spherical stress is greater than that of generalized shear stress. Meanwhile, by comparing Figs. 1 (a)–(d), it can be seen that the effective stress ratio decreases with increasing net confining pressure.

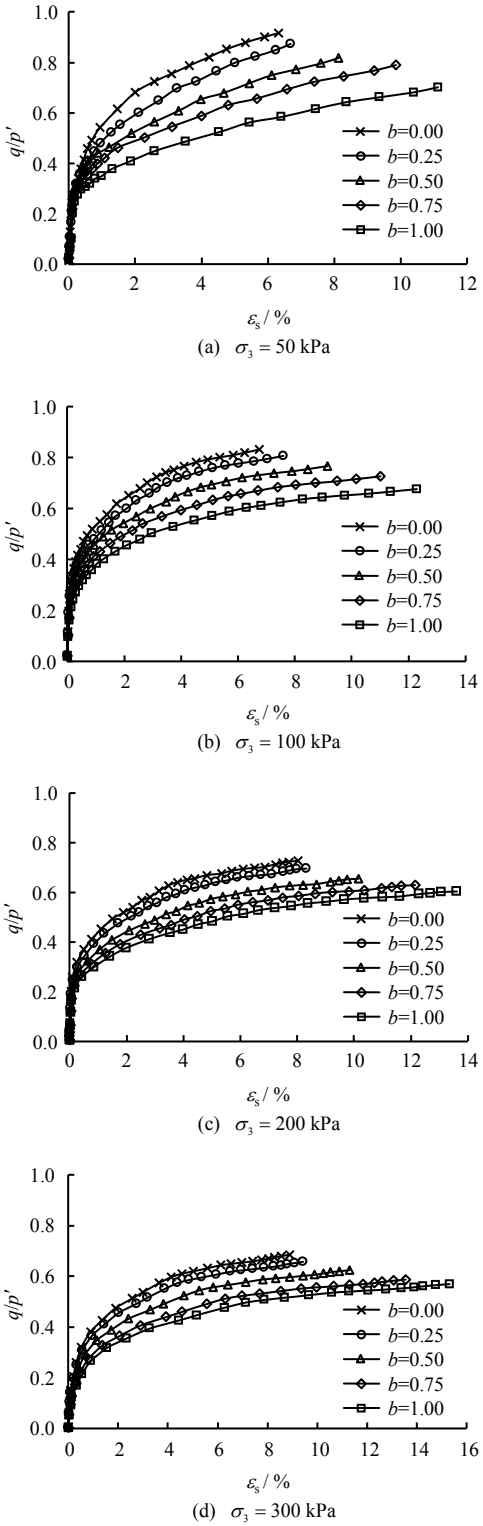

(a) σ_3 = 50 kPa

(b) σ_3 = 100 kPa

(c) σ_3 = 200 kPa

(d) σ_3 = 300 kPa

Fig.1 q/p'-ε_s relationship curves

3.1.2 The relationship between effective stress ratio and volumetric strain

Figure 2 shows the ε_v–lg(q/p') curves, which are relationship between effective stress ratio and volumetric strain under true triaxial shear for unsaturated intact loess (s_0 = 170 kPa). When the net confining pressure σ_3 is constant, the ε_v–lg(q/p') curve moves upward to the left with the increase of b value, which demonstrates that when lg(q/p') is constant, the volumetric strain of soil increases with increasing b value. By comparing Figs.2 (a)–(d), the volumetric strain of soil increases with increasing σ_3. Meanwhile, according to the method of Chen[16], the yield point of effective stress space can be determined by the intersection point of two straight lines on the ε_v–lg(q/p') curve, and the stresses (q'_y, p'_y) of yield point are the yield stresses, as shown in Fig.2. When σ_3 is constant, the yield point moves towards the upper left side with increasing b value.

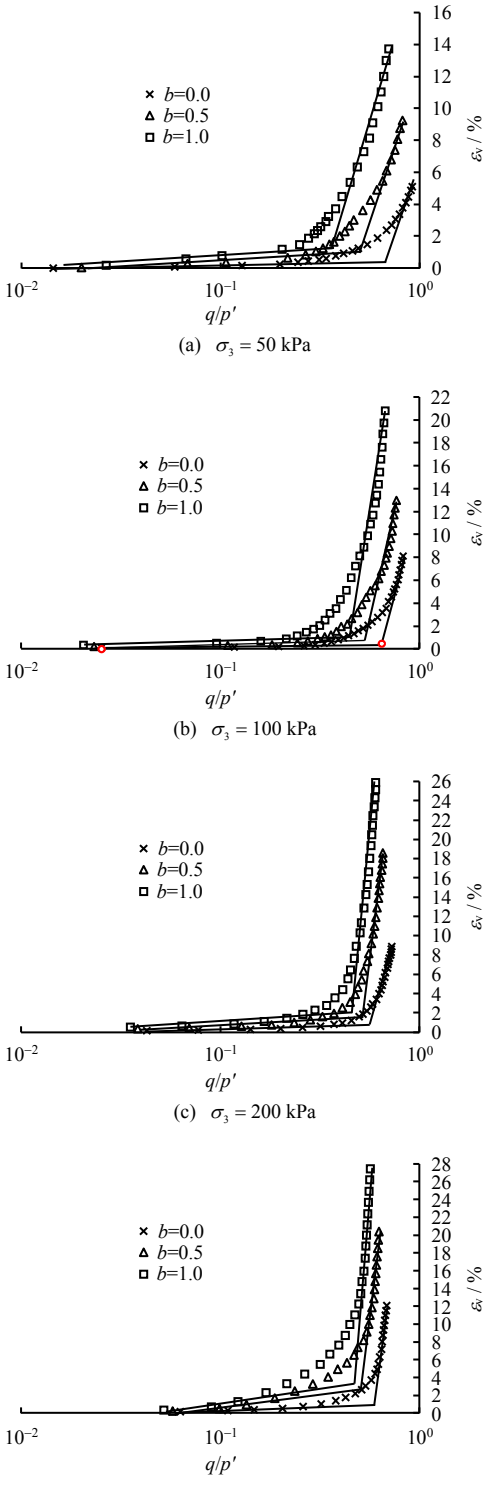

(a) σ_3 = 50 kPa

(b) σ_3 = 100 kPa

(c) σ_3 = 200 kPa

(d) σ_3 = 300 kPa

Fig.2 ε_v -lg(q/p') relationship curves

Which is, ε_v increases and lg(q/p') decreases, indicating that the increase of b value has greater influence on the effective spherical stress than on the generalized shear stress.

3.2 Change of effective stress shear yield strength

3.2.1 Relationship between the generalized shear stress and average effective spherical stress in the shear yield state

According to the method shown in Fig.2, the yield stress (q'_y, p'_y) of yield point in the effective stress space for unsaturated intact loess can be determined. Figure 3 shows the p'-q relationship curves between generalized shear stress and average effective spherical stress at the shear yield state for unsaturated undisturbed loess. As can be seen from Fig.3:

Under true triaxial shear condition, the p'-q curves between generalized shear stress and average effective spherical stress in the shear yield state are all in curvilinear pattern, this is due to the destruction of original soil structure with the increase of effective spherical stress, and the yield shear stress of soil is reduced [14].

By comparing Fig.3 (a) and (b), the effective yield stress (q'_y, p'_y) of the soil rises with the increase of b value. It draws the conclusion that effective yield stress of unsaturated soil is related to the intermediate principal stress. This is because on the one hand , the compression strength of the soil is strengthened with the increase of b value, hence the ability to resist the deformation of the soil is strengthened. On the other hand, the vertical structure of the soil is enhanced, so the effective yield stress of the soil is greater [14].

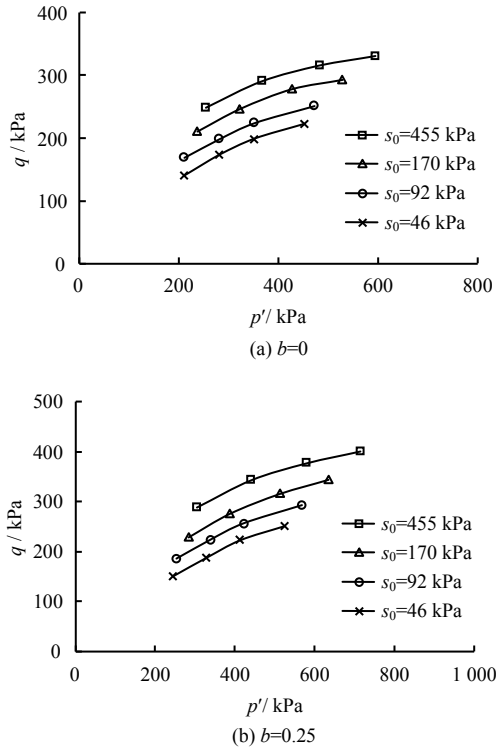

Fig.3 Yield curves in the p'-q plane under true tri-axial shear

When the b value is constant, the effective yield stresses exhibited by the yield curves rise with increase of initial suction s_0, which indicates that the yield effective spherical stress and yield shear stress increase with the increase of s_0 under true triaxial shear condition. This is because the larger the s_0, the smaller the water content, the stronger the structure and better capacity to withstand higher compression and shear. In addition, the effect of suction can improve the structural stability of soil skeleton [14,17–23].

From the above analysis, it can be seen that the shear shrinkage yield curves determined by the curves between effective stress ratio and volumetric strain under true triaxial shear have good regularity in the effective stress space. The effective yield stress of yield point increases with increasing intermediate principal stress and initial suction. When the b value is constant, the yield curve tends to expand outward with the increase of initial suction.

3.2.2 Variation of shear shrinkage yield strength of effective stress on the π plane

Figure 4 shows the effective stress yield strength surfaces on the π plane, where the hollow points are test points and the solid lines are theoretical lines. It can be seen from Fig.4 that the effective stress yield strength surfaces of unsaturated intact loess are similar in shape on the π plane, and can be approximately fitted by the SMP strength criterion. It can be seen from Figs.4(a) and (b) that when the initial suction is constant, the yield strength surface of soil tends to expand outward with the increase of the effective spherical stress, indicating that the larger the effective spherical stress, the greater the yield strength. As shown in Fig.4 (c), when the effective spherical stress is constant, the yield strength surface of soil tends to expand outwards with increase of initial suction, indicating that the larger the initial suction, the greater the yield strength. Figure 4(d) shows the yield strength surfaces of each strength criterion on the π plane when s_0 = 455 kPa, p' = 400 kPa. It can be seen that the yield strength based on different strength criteria in the descending order are Mises criterion, Treasa criterion, SMP criterion and Mohr-Coulomb criterion. The test points in this paper are coincident with SMP strength criterion, which shows that SMP strength criterion can well describe the yield strength of unsaturated intact loess at different intermediate principal stress ratios under true triaxial condition. Matsuoka studied the strength criterion on SMP, which can consider the influence of intermediate principal stress on the soil strength[24]. It is connected to six corners of Mohr-Coulomb criterion on the π plane. Treasa criterion has no relation with hydrostatic pressure. It is not suitable for the soil materials with frictional property, and does not consider the effect of intermediate principal stress. It is a regular hexagon on

the π plane. Mises criterion is a constant distortion energy theory, which has no relation with hydrostatic pressure. It cannot describe the change of soil strength with Lode angle, and appears as circumcircle of Treasa criterion on π plane. Mohr–Coulomb criterion does not consider the influence of intermediate principal stress, and there are singular points on the failure surface, which is difficult to deal with in the numerical analysis. It is a hexagon with unequal angle on π plane.

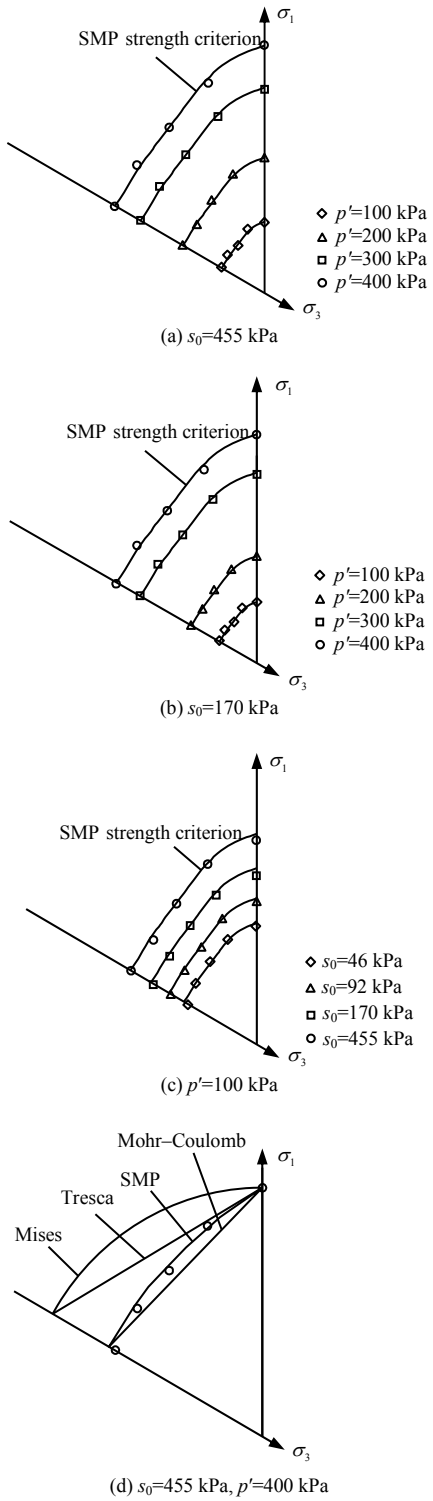

Fig.4 The effective stress yield strength line of π plane

3.3 Variation of shear failure strength of effective stress

3.3.1 Relationship between the generalized shear stress and the average effective spherical stress in shear failure state

Figure 5 shows the failure state line of unsaturated intact loess on the *p*'-*q* plane under different *b* values. It can be seen that when the *b* value is constant, the test points of unsaturated intact loess with different initial suctions are all in a narrow distribution band on the *p*'-*q* plane, and can be approximated to a straight line passing the origin. In reference [25], when $b = 0$, the failure state line on the *p*'–*q* plane is also a straight line passing through the origin. Therefore, under different *b* values, the failure state line of unsaturated intact loess on the effective stress *p*'–*q* plane can be approximated to a straight line past the origin. At the same time, by comparing Figs.5(a) with (b), it is found that the effective spherical stress and the failure strength of soil increase correspondingly with the increase of intermediate principal stress.

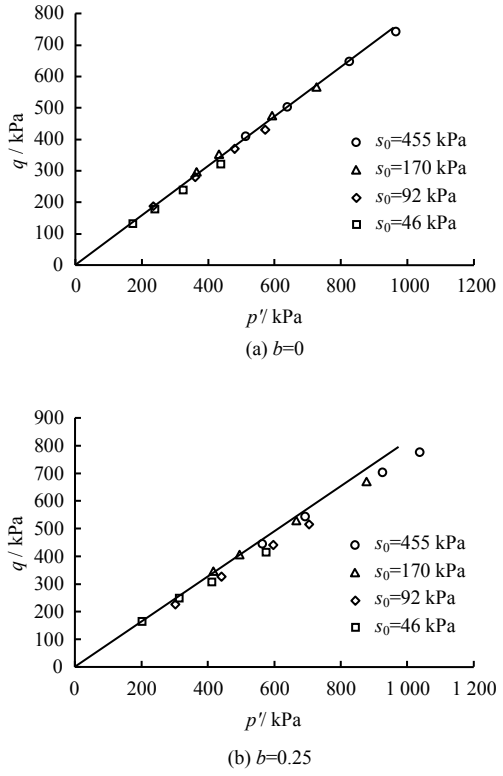

Fig.5 The damage state line of *p′*-*q* plane

3.3.2 Variation of shear failure strength of effective stress on π plane

Figure 6 shows the effective stress strength failure surfaces on the π plane, where the hollow points are test points and the solid lines are theoretical lines. It can be seen from Fig.6 that the effective stress strength failure surfaces of unsaturated intact loess on the π plane are similar in shape, which can be approximately fitted by the SMP strength criterion. When the initial suction is constant, the effective stress strength failure

surface of soil tends to expand outward with the increase of effective spherical stress, indicating that the larger the effective spherical stress, the greater the strength failure surface. By comparing Fig.6 (a) and (b), it is indicated that when the initial suction is greater, the effective stress strength failure surface of soil is larger. Meanwhile, as shown in Fig.6 (c), when the effective spherical stress is constant, the effective stress strength failure surface of soil tends to expand outward with the increase of the initial suction, indicating that the greater the initial suction, the larger the effective stress strength failure surface.

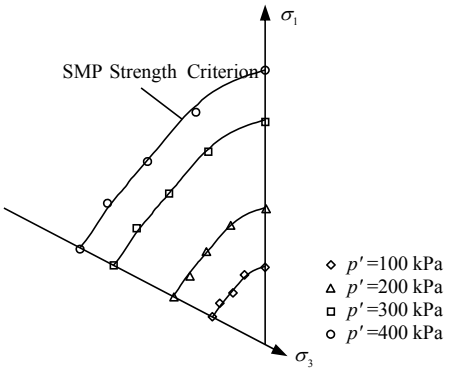

(a) s_0 = 455 kPa

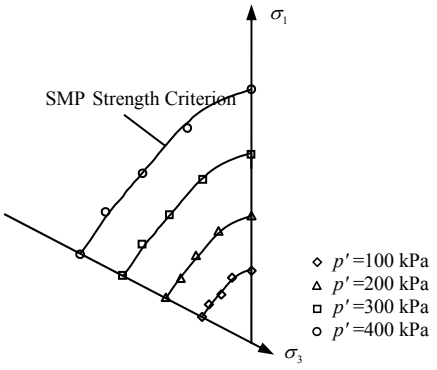

(b) s_0=170 kPa

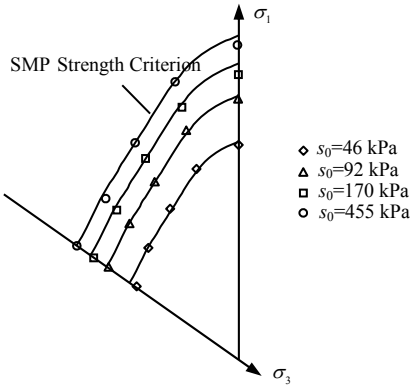

(c) p'=100 kPa

Fig.6 The effective stress strength failure surface on π plane

3.4 The law of shear yield hardening in different meridian planes of effective stress space

Huang et al.[26–27] believed that the yield surface of soil should not be assumed, and the plastic potential function should be directly determined by specific experimental data. The appropriate hardening parameter should be chosen to make the yield function and plastic potential function equal, so as to satisfy the associated flow rule, thus the elastoplastic constitutive model of soil is established. In this paper, the determining methods for yield function and plastic potential function in effective stress space are as follows: The elastic strain and plastic strain were separated from the test curve by conventional triaxial test and isotropic compression test. Assuming that pure shear does not cause elastic volumetric strain ε_v^e, that is, the elastic volumetric strain increment $\mathrm{d}\varepsilon_v^e$ is caused by effective spherical stress increment $\mathrm{d}p'$. And then, the elastic volumetric strain ε_v^e can be obtained from the unloading section of the relation curve $\varepsilon_v - \ln p'$ by isotropic compression tests, that is

$$\varepsilon_v^e = \frac{\kappa}{1+e_0}\ln\frac{p'_x}{p'_0} \tag{3}$$

where κ is the slope of the curve of the rebound and reloading section; p'_x is the effective spherical stress applied; p'_0 is the effective spherical stress corresponding to the initial void ratio. At the same time, the plastic volumetric strain ε_v^p and plastic shear strain ε_s^p can be obtained as follows:

$$\varepsilon_v^p = \varepsilon_v - \varepsilon_v^e \tag{4}$$

$$\varepsilon_s^p = \varepsilon_1 - \frac{1}{3}\varepsilon_v^p \tag{5}$$

The Eq. (5) is suitable for the case of intermediate principal stress parameter b=0. When b≠0, the elastic shear strain ε_s^e can be obtained by the generalized Hooke's law:

$$\varepsilon_s^e = \frac{2(1+\mu)}{3E}q \tag{6}$$

where $E = 3(1-2\mu)\dfrac{1+e}{\kappa}p'$; μ is the Poisson's ratio, $\mu = 0.3$. In this paper, $\kappa = 0.007$.

Then, when $b \neq 0$, the plastic shear strain ε_s^p is

$$\varepsilon_s^p = \varepsilon_s - \varepsilon_s^e \tag{7}$$

Figure7 shows the p– ε_v^p and q– ε_s^p relation curves of unsaturated intact loess (s_0=170 kPa) under different b values. It can be seen that the p' - ε_v^p relation curve rises with the increase of net confining pressure, indicating that when ε_v^p is constant, effective spherical stress increases with the increase of net confining pressure. By comparing Figs.7 (a)–(d), it can be

seen that with the increase of b value, both the effective spherical stress and the plastic volumetric strain rise correspondingly. At the same time, the curve of $q-\varepsilon_s^p$ relation is approximately hardening curve when the value of b is constant, and the generalized shear stress of soil increases with the increase of net confining pressure and b value.

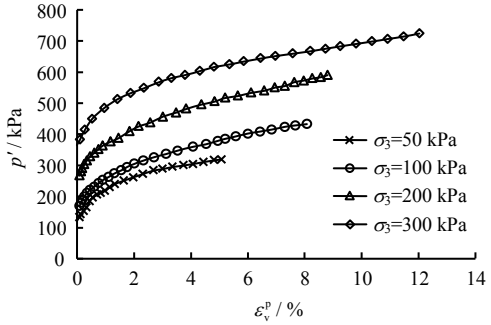

(a) $p'-\varepsilon_v^p$ curves at b=0

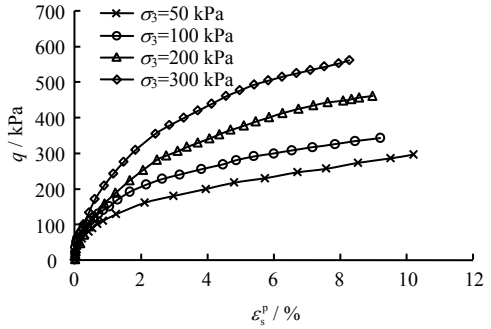

(b) $q-\varepsilon_s^p$ curves at b=0

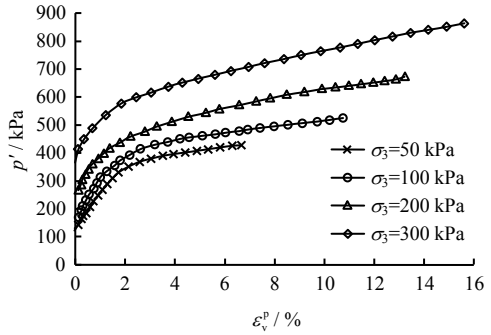

(c) $p'-\varepsilon_v^p$ curves at b=0.25

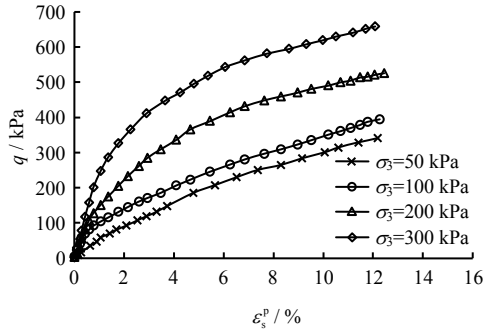

(c) $q-\varepsilon_s^p$ curves at b=0.25

Fig.7 p'- ε_v^p and q- ε_s^p relationship curves

The obtained plastic volumetric strain and plastic shear strain are plotted on the p'-q plane, and then the strength line is constructed on the p'-q plane. Figure 8 shows the yield surfaces of unsaturated intact loess (s_0=170 kPa) in effective stress space under different b values. In this paper, the plastic volumetric strain is taken as the hardening parameter, the ε_v^p axis and the ε_s^p axis are coincident with the p' axis and the q axis, respectively. The any point $M(p',\ q)$ of p'-q plane is represented by vectors ε_v^p and ε_s^p, which can be synthetized to obtain the direction of plastic strain increment, such as the direction of small arrowheads in Fig.8. The streamline clusters in Fig.8 can be drawn in the direction of connecting the points. Finally, the lines orthogonal to the streamline clusters are made, that is, the locus of plastic potential line are obtained. It can be seen from Fig.8, the plastic potential locus in the effective stress space under different b values are ellipses orthogonal to the p' axis, which is consistent with the conclusion that the plastic potential locus in the effective stress space is an ellipse under conventional triaxial condition (i.e.b=0)[10–11]. However, by comparing Figs. 8 (a)–(e), it can be seen that the elliptical yield surface increases with increasing b value. The results show that intermediate principal stress has an effect on the unsaturated loess yield surface in the effective stress space. The larger the intermediate principal stress is, the larger the elliptical yield surface is.

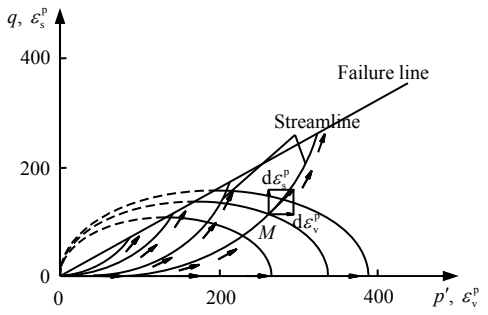

(a) b=0

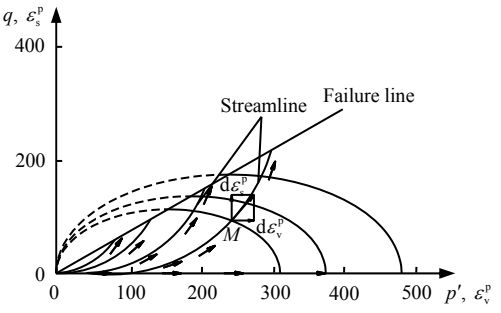

(b) b=0.25

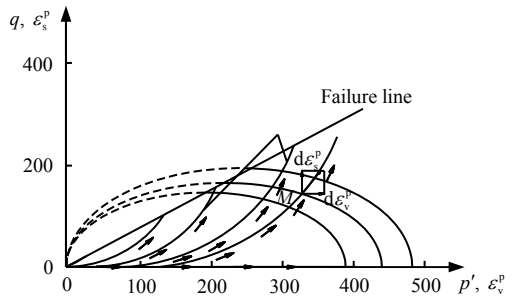

(c) b=0.5

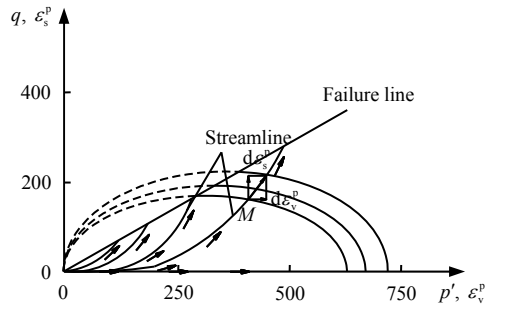

(d) b=0.75

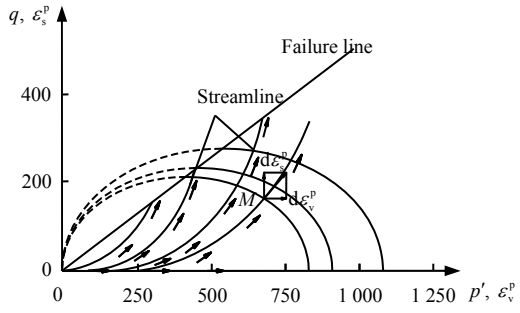

(e) b=1

Fig.8 The plastic potential lines of intact loess for s_0 = 170 kPa

4 Conclusions

(1) The effective stress ratio of unsaturated soil reduces with the increase of net confining pressure or intermediate principal stress. When the net confining pressure is constant, the effective stress ratio rises with the increase of generalized shear strain under different intermediate principal stress condition. The effect of intermediate principal stress on the effective spherical stress is greater than that of the generalized shear stress.

(2) The shear shrinkage yield curves determined by the curves between effective stress ratio and volumetric strain under true triaxial shear have good regularity in the effective stress space. The effective yield stress of yield point increases with increase of intermediate principal stress and initial suction. When the b value is constant, the yield curve tends to expand outward with the increase of initial suction.

(3) The effective stress yield strength surface and strength failure surface of unsaturated intact loess on the π plane reflect the effect of intermediate principal stress on soil strength well. It is coincident with SMP strength criterion. The greater the effective spherical stress and initial suction, the larger the yield strength surface and the strength failure surface.

(4) Under true triaxial condition of different intermediate principal stresses, the failure state line of unsaturated intact loess on the effective stress p'-q plane is approximately a straight line passing through the origin. With increasing intermediate principal stress, the effective spherical stress and the soil failure strength increase correspondingly.

(5) The formulas of elastic shear strain and plastic shear strain are put forward under true triaxial condition. The plastic volumetric strain of unsaturated intact loess increases with increasing intermediate principal stress. Under different intermediate principal stress condition, the q-ε_s^p relation curve is approximately hardening curve. By analyzing the relationship between true triaxial stress and plastic strain, it is found that the plastic potential surface in different meridional planes in the effective stress space is elliptical, and the elliptical yield surface enlarges with the increase of intermediate principal stress.

References

[1] TERZAGHI K V. Die berechnung der durchlassigkeitsziffer des tones aus dem verlauf der hydrodynamischen spannungserscheinungen[J]. Sitzungber Akad Wiss Wien, 1923, 132: 125–138.

[2] BISHOP A W. The principle of effective stress[J]. Teknisk Ukeblad, 1959, 106(39): 113–143.

[3] JENNINGS J E B, BURLAND J B. Limitations to the use of effective stresses in unsaturated soils[J]. Geotechnique, 1962, 12: 125–144.

[4] COLEMAN J D. Stress-strain relations for partly saturated soils[J]. Geotechnique, 1962, 12(4): 348–350.

[5] BISHOP A W, BLIGHT G E. Some aspects of the effective stress in saturated and partially saturated soils[J]. Geotechnique, 1963, 13(3): 177–197.

[6] BLIGHT G E. Effective stress evaluation for unsaturated soils[J]. Journal of the Soil Mechanics and Foundations Division, ASCE, 1967, 93(SM2): 125–148.

[7] FRELUND D G, MORGENSTERN N R. Stress state variables for unsaturated soils[J]. Journal of Geotechnical Engineering Division, ASCE, 1977, 103(5): 447–466.

[8] WHEELER S J, SHARMA R S, BUISSON M S R. Coupling of hydraulic hysteresis and stree-strain behaviour in unsaturated soils[J]. Geotechnique, 2003, 45(1): 35–53.

[9] BOLZON G, SCHREFLER B A, ZIENKIWICZ O C. Elastoplastic soil constitutive laws generalised to partially saturated states[J]. Geotechnique, 1996, 46(2): 279–289.

[10] MIAO Lin-chang. Research on constitutive model of unsaturated soils[J]. Rock and Soil Mechanics, 2007, 28(5): 855–860.

[11] SUN De-an. Hydro-mechanical behaviours of unsaturated soils and their elastoplastic modeling[J]. Rock and Soil Mechanics, 2009, 11(30): 3217–3231.

[12] CHEN Cun-li, ZHANG Deng-fei, DONG Yu-zhu, et al. Suction and mechanical behaviours of unsaturated intact loess from constant water content triaxial tests[J]. Chinese Journal of Geotechnical Engineering, 2014, 36(7): 1195–1202.

[13] SHAO Sheng-jun, LUO Ai-zhong, DENG Guo-hua. Development of a new true tri-axial apparatus[J]. Chinese Journal of Geotechnical Engineering, 2009, 31(8): 1172–1179.

[14] FANG Jin-jin, SHAO Sheng-jun, LI Rong, et al. Yield characteristics of Q_3 loess in true triaxial tests[J]. Chinese Journal of Rock Mechanics and Engineering, 2016, 35(9): 1936–1944.

[15] FANG Jin-jin, SHAO Sheng-jun, FENG Yi-xin. Suction changes of intact Q_3 loess based on true triaxial tests[J]. Rock and Soil Mechanics, 2017, 38(4): 934–942.

[16] CHEN Zheng-han. Deformation, strength, yield and moisture change of a remolded unsaturated loess[J]. Chinese Journal of Geotechnical Engineering, 1999, 21(1): 82–90.

[17] XIE Ding-yi, QI Ji-lin. Soil structure characteristics and new approach in research on its quantitative parameter[J]. Chinese Journal of Geotechnical Engineering, 1999, 21(6): 651–656.

[18] XIE Ding-yi, QI Ji-lin, ZHU Yuan-lin. Soil structure parameter and its relations to deformation and strength[J]. Journal of Hydraulic Engineering, 1999(10): 1–6.

[19] SHAO Sheng-jun, ZHOU Fei-fei, LONG Ji-yong. Structural properties of loess and its quantitative parameter[J]. Chinese Journal of Geotechnical Engineering, 2004, 26(4): 531–536.

[20] SHAO Sheng-jun, WANG Li-qin, TAO Hu, et al. Structural index of loess and its relation with granularity, density and humidity[J]. Chinese Journal of Geotechnical Engineering, 2014, 36(8): 1387–1393.

[21] DANG Jin-qian, LI Jing. Structure strength and shear strength of unsaturated loess[J]. Journal of Hydraulic Engineering, 2001, 7(7): 79–84.

[22] LUO Ya-sheng, XIE Ding-yi, LI Peng. Main influence factors on structural property changes of unsaturated loess[J]. Bulletin of Soil and Water Conservation, 2005, 25(2): 36–39.

[23] CHEN Cun-li, HE Jun-fang, YANG Peng. Constitutive relationship of intact loess considering structural effect[J]. Rock and Soil Mechanics, 2007, 28(11): 2284–2290.

[24] LUO Ting, YAO Yang-ping, HOU Wei. Constitutive relation of soils[M]. Beijing: China Communications Press, 2010.

[25] NUTH M, LALOUIL. Effective stress concept in unsaturated soils: clarification and validation of a unified framework[J]. International Journal for Numerical and Analytical Methods in Geomechanics, 2008, 32(7): 771–801.

[26] HUANG Wen-xi, PU Jia-liu, CHEN Yu-jiong. Hardening rule and yield function for soils[J]. Chinese Journal of Geotechnical Engineering, 1981, 3(3): 19–26.

[27] HUANG Wen-xi. Theory of elastoplastic stress-strain models for soils[J]. Rock and Soil Mechanics, 1979, 12(2): 1–26.